Carbon Letters (2020) 30:683–698
https://doi.org/10.1007/s42823-020-00141-1

Online ISSN 2233-4998
Print ISSN 1976-4251

ORIGINAL ARTICLE

Heavy metal ions (lead, cobalt, and nickel) biosorption from aqueous solution onto activated carbon prepared from *Citrus limetta* leaves

Elham Aboli[1] · Dariush Jafari[2] · Hossein Esmaeili[2]

Received: 24 August 2019 / Revised: 10 March 2020 / Accepted: 23 March 2020 / Published online: 31 March 2020

Abstract

In this research, Pb (II), Co (II), and Ni (II) toxic heavy metal ions adsorption from synthetic aqueous system have been studied using the activated carbon prepared from *Citrus limetta* leaves. Therefore, the relationship between the adsorption parameters (solution pH, dosage of adsorbent, temperature, initial concentration of the ions, and adsorption time) and the removal percentage of the prepared adsorbent have been investigated. Additionally, the adsorbent was analyzed through BET, SEM, EDX, FTIR, and XRD analyses. According to the results, the maximal adsorption efficiencies for heavy metal ions were achieved in pH = 6, the adsorbent dosage of 1 g/L, temperature = 25 °C, the ion initial concentration of 5 mg/L, and contact time of 60 min, which were 99.53%, 98.63%, and 97.54% for Pb, Co, and Ni ions, respectively. Based on Kinetic studies, the performance of pseudo-second-order kinetic model was better than pseudo-first-order model for the description of time-dependent behavior of the process. Additionally, the equilibrium data were fitted by Langmuir and Freundlich isotherms, while the former performed better than the latter. The maximum adsorption capacity values for Pb, Co, and Ni ions were achieved equal to 69.82, 60.60, 58.139 mg/g, respectively. Considering the thermodynamic data, the studied processes were exothermic and spontaneous.

Keywords Heavy metals ions · *Citrus limetta* leaves · Adsorption · Activated carbon · Kinetic behavior

Abbreviations

C_i	Initial concentration of metal ions (mg/L)
C_e	Equilibrium concentration of metal ions (mg/L)
K_1	Pseudo-first-order model rate constant (1/min)
K_2	Pseudo-second-order kinetic rate constant ($g.mg^{-1}.g^{-1}$)
K_e	Adsorption equilibrium constant
K_f	Freundlich model constant (L/mg)
K_L	Adsorption energy (L/mg)
n	Freundlich model constant
q_e	Equilibrium capacity (mg/g)
q_{max}	Maximum adsorption capacity (mg/g)
q_t	The value of the adsorbed ion per gram of adsorbent at time t (mg/g)
R	Universal gas constant (J/mol·k)
$\%R$	Adsorption efficiency
R_L	Adsorption intensity
T	Absolute temperature (K)
t	Time (minutes)
V	Volume of solution (L)
W	Adsorbent mass (g)
$\Delta G°$	Gibbs free energy (kJ/mol)
$\Delta H°$	Enthalpy (kJ/mol)
$\Delta S°$	Entropy (J/mol.K)

Electronic supplementary material The online version of this article (https://doi.org/10.1007/s42823-020-00141-1) contains supplementary material, which is available to authorized users.

✉ Dariush Jafari
dariush.jafari@yahoo.com

[1] Department of Chemical Engineering, School of Chemical Engineering, Kherad Institute of Higher Education, Bushehr, Iran

[2] Department of Chemical Engineering, Bushehr Branch, Islamic Azad University, Bushehr, Iran

1 Introduction

Environment protection and especially the treatment of wastewaters are very important issues in scientific and industrial societies since the emission of industrial wastes have irreparable and fatal impacts on the environment and human life by threatening to the ecological balance [1]. Among the various pollutants, Heavy metals are considered as chemicals which are non-biodegradable. Therefore

these ions can cause health risks, since they enter the human food chain through the adsorption by water and soil [2–5]. Lead is one of the toxins which is released into the surface waters from various industries producing batteries, dye and paint, cable, steel, plastic, and oil industry [6–8]. The maximum permissible concentration of Pb(II) ion in potable water is 0.05 mg/L [9]. Nickel is another toxic heavy metal ion that has been emitted in the environment as the result of operations like plating, mining, and battery production [10]. The presence of excess Ni(II) ions in drinking water results in higher risks of diseases like lung and bone cancer. Acute poisoning by nickel is accompanied by headache, nausea, weakness, dry coughs, and pain in chest [11]. Cobalt is found in the form of various salts in the environment. It has been abundantly used in nuclear medicine and production of glazes, semi-conductors, resin stabilizers, paints and polishes, and plating industry. Adverse health effects are reported due to extreme exposure to high concentrations of Co such as hypotension, lung diseases, paralysis, and bone defects and also genetic mutations. To minimize the environmental impacts of heavy metal ions, several techniques have been applied to remove them from wastewaters including chemical sedimentation, coagulation, membrane method, electrolyte reduction, and ion exchange [12–14]. However, some of their high operational costs and also their probable low removal efficiencies at trace level concentrations of toxic metal ions limited the application of these mentioned techniques [15]. Adsorption method has been extensively used for the treatment of wastewaters recently [16]. The application of low-cost adsorbents produced from agricultural wastes, clays, biomass, and marine products has become an important option in the field of wastewater treatment [17]. One of the most common and effective adsorbents is activated carbon which presents excellent porosity and specific surface area [18]. Several researches have been performed on the application of these low-cost adsorbents produced from cheap agricultural wastes [19–26]. *Citrus limetta* tree is abundantly cultivated in the south of Iran, which makes it as a proper source of activated carbon bioadsorbents.

This study was set out to convert the *Citrus limetta* leaves to useful and value-added activated carbon adsorbent to evaluate its adsorption potential for lead, cobalt, and nickel ions removal from aqueous solution through the variation of some process parameters like solution pH, the dosage of adsorbent, temperature, ions initial concentration, and adsorption time. Additionally, the prepared activated carbon was characterized using BET, SEM, EDX, FTIR, and XRD analyses. The achieved adsorption data were analyzed to study the equilibrium, kinetic, and thermodynamic of the mentioned ions adsorption.

2 Materials and methods

2.1 Chemicals

Sodium hydroxide, hydrochloric acid, lead (II) nitrate ($Pb(NO_3)_2$), cobalt (II) nitrate ($Co(NO_3)_2$), and nickel (II) nitrate ($Ni(NO_3)_2$) were purchased from Merck Company (Germany) with the purity of > 99%. In addition, Pb (II), Co (II), and Ni (II) solutions were prepared using double distilled water in all of the adsorption experiments.

2.2 Preparation of stock solution

To prepare the stock solutions 0.16 g of $Pb(NO_3)_2$, 0.5 g $Co(NO_3)_2$, and 0.617 of $Ni(NO_3)_2$ were dissolved in double-distilled water in three separate 100-mL volumetric flasks. Thereafter the stock solutions were diluted by distilled water to have 5–100 ppm solutions of the ions It is worth noting that pH adjustment of the prepared samples was done using sodium hydroxide and hydrochloric acid (1 M).

2.3 Adsorbent preparation and characterization

In the current research, the leaves of *Citrus limetta* were collected from the local gardens of Boushehr province (Iran) as the resource of activated carbon. The collected leaves were initially washed carefully by distilled water to remove dust and other impurities. Then the leaves were dried by and oven for 24 h in 100 °C. Afterwards, the dried leaves were placed in a nitrogen atmosphere furnace in 700 °C for 3 h to convert into activated carbon under nitrogen atmosphere in the heating rate of 0–20 °C/min. The carbonized material was powdered using an electric grinder and then sieved by sieve no. 25 to obtain a powder of uniform particle size. The prepared activated carbon powder was stored in tightened cap glass bottles for further characterization and adsorption experiments.

In the current study, BET (Belsorp, Belsorp mini II, Japan), SEM (Tisteam MIRA III, Czech Republic), FTIR (Tensor II Bruker, Germany), EDX (Tisteam SAM), and XRD (Netherland, X-pert- proma D Panalytical) analyses were performed to determine the specific surface are of adsorbent, its structure and morphology, the surface functional groups of the adsorbent, elements present in its structure and their corresponding weight percentages, and the adsorbent crystallinity, respectively.

2.4 Adsorption experimental procedure

As mentioned before, in this research the effects of adsorption parameters like pH (3–11), dosage of adsorbent

(0.25–1.5 g/L), temperature (25–50 °C), metal ions initial concentration (5–100 mg/L), and contact time (5–120 min) were evaluated for determination of uptake efficiencies of Pb(II), Co(II), and Ni(II) ions from the synthetic aqueous solutions by the prepared activated carbon from *Citrus limetta* leaves. To attain the significance of solution pH in the above-mentioned range, the adsorption experiments were conducted in a series of Erlenmeyer flasks containing solutions with the following conditions: adsorbent dosage of 0.75 g/L, cadmium initial concentration of 40 ppm, the temperature of 25 °C, 60 min as the adsorption time, and stirring rate of 200 rpm. After the end of each experiment, the samples were filtered using Whatman grade 42 filter paper and the remained solution was analyzed using flame atomic adsorption device (VARIAN, USA) to determine the residual cadmium ions in the solution. To achieve the optimum values of other parameters, pH should be fixed in the prior optimized value while the effect of others were investigated in their corresponding ranges. Using Eq. (1), the adsorption efficiency (%*R*) of the ions were calculated:

$$R\,(\%) = \frac{C_i - C_e}{C_i} \times 100, \tag{1}$$

where, C_i (mg/L), is the initial concentration and C_e (mg/L) is the equilibrium concentration of the metal ions.

The equilibrium adsorption capacity (mg/g) was determined by Eq. (2):

$$q_e = \frac{\left(C_i - C_e\right)}{w} \times V. \tag{2}$$

In this equation, V is the volume of solution (L) and W is the adsorbent mass (g).

3 Results and discussion

3.1 Characterization of the activated carbon

The produced activated carbon adsorbent from *Citrus limetta* leaves was characterized by various techniques. BET analysis indicated that specific surface area, the volume of the pores, and adsorbent cavities average diameter were 7.2 m^2/g, 0.0168 cm^3/g, and 24.8 nm, respectively. The adsorption/desorption isotherm curve of the prepared activated carbon is shown in Fig. 1.

SEM analysis was used to study the pore and surface morphology variations of the prepared activated carbon before and after the adsorption of ions. Based on SEM images presented in Fig. 2a, the prepared adsorbent surface was porous with a large number of pores on its surface which makes it appropriate for the removal of impurities. Additionally, Fig. 2b–d which are the SEM micrographs of the adsorbent after the removal of Pb, Co, and Ni ions, show that the surface pores were approximately covered as the result of adsorption of mentioned ions.

EDX analysis results (Fig. 3 and Table 1) show that elements including carbon, iron, oxygen, aluminum, phosphor, calcium, sulfur, magnesium, silicon, sulphur, and potassium were present in the prepared adsorbent. Additionally, after the adsorption of lead, cobalt, and nickel ions, it can be observed that these elements appeared in the output of EDX analysis, which denotes that these ions were adsorbed by the current adsorbent. Additionally, carbon has been one of the most main constituents of the activated carbon analyzed samples. As shown in Table 1, the weight percentages of Pb(II), Co(II), and Ni(II) ions in the activated carbon structure were 4.79%, 4.34%, and 10.12%, respectively. This means that these ions have been attached to the prepared activated carbon active sites through the adsorption process. The figures also denote the higher tendency of the adsorbent prepared from *Citrus limetta* leaves to remove nickel ions from the aqueous solution in comparison with the other two ions.

FTIR images of the prepared adsorbent before and after the adsorption of Pb(II), Co(II), and Ni(II) ions are presented in Fig. 4. As it can be observed there are two peaks at 872 cm^{-1} and 711 cm^{-1} which correspond to S–S and S–OR vibrations, that is reported in previous studies [27]. The peaks that are appeared in the frequency range of 1427 cm^{-1} are related to tension vibrations of C–C functional group which are shifted to 1406, 1407, 1406 cm^{-1} after lead, cobalt, nickel adsorption [28, 29]. Additionally, the peaks that are observed in the spectra range of 1795 cm^{-1} can be associated with C=O group [30]. There is a peak in the frequency range of 1028–1034 cm^{-1}, which is related to the deformation of aromatic –CH group [31]. Figure 4a shows two peaks at 616 cm^{-1} and 1110 cm^{-1} that are associated with Mg–O/Al–O and –C–O groups, which disappeared after the adsorption of ions [32]. There is also a peak at 2081 cm^{-1} (dicarbonyl) which is appeared after the removal of these three ions [33]. Furthermore, the peak at the wavenumber of 2325 cm^{-1} shifted to 2388 cm^{-1} due to the removal of heavy metal ions.

The crystallinity of the prepared activated carbon from *Citrus limetta* leaves was evaluated through XRD analysis and its results are presented in Fig. 5. The peaks that are observed in 2θ values of 23°, 31°, and 43.27° can be associated to (002) and (001) crystalline phases of graphite structure [34]. It is worth noting that according to previous researches, the peaks that were appeared in $2\theta = 43°$ can be related to (100) and (101) crystalline phases which confirm graphite structure of the prepared activated carbon [35, 36]. Considering these XRD spectra, it can be concluded that the current adsorbent had a crystalline structure and no significant changes were seen in the location and intensity of

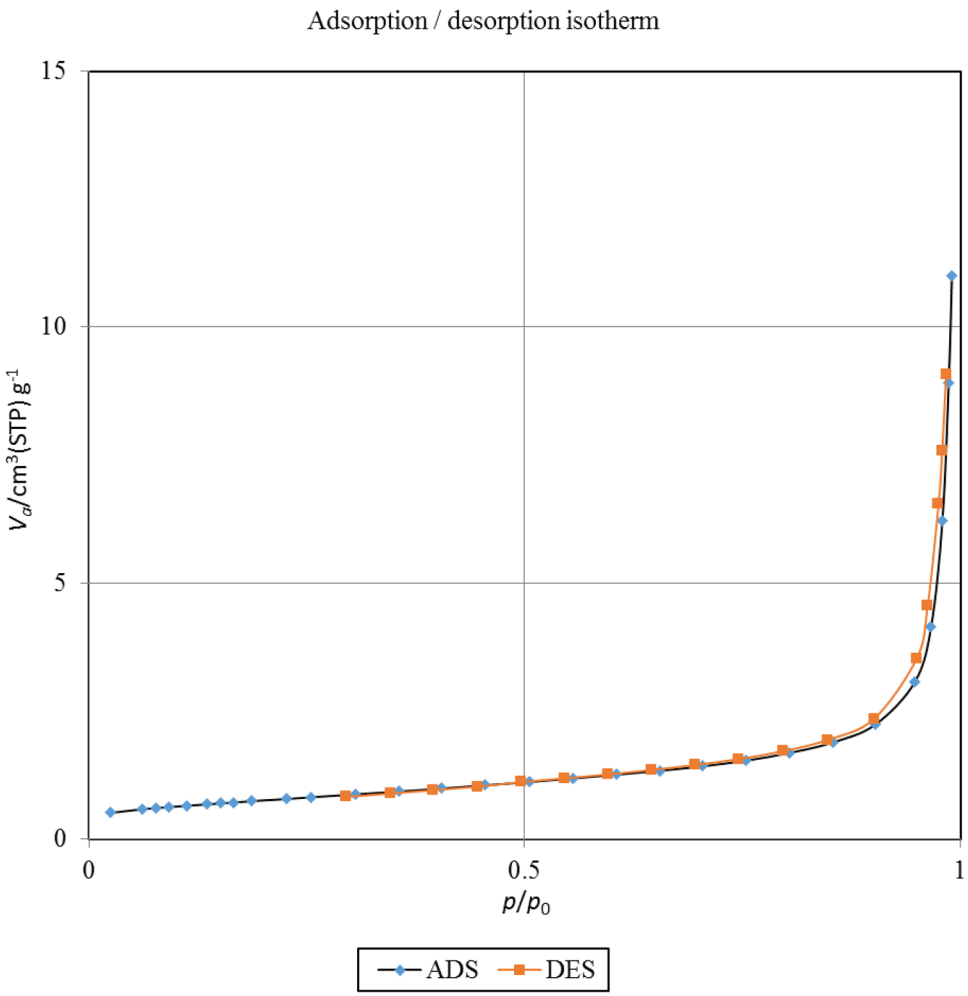

Fig. 1 BET Adsorption/desorption isotherm curve of the prepared activated carbon

activated carbon structure XRD peaks after the metal ion adsorption. Therefore, the adsorbent had retained its crystalline structure after the adsorption of lead, cobalt, and nickel ions.

3.2 Effect of solution pH

Solution pH is an effective component in adsorption processes [37]. Figure 6 indicates the effects of solution pH on heavy metal ions removal efficiency. According to this figure, there is a positive correlation between pH and the ions uptake efficiencies in the range of 3–6, since lead, cobalt, and nickel ions adsorption efficiencies increased from 47.56% to 97.84%, 43.78% to 95.62%, and 38.42% to 93.43%, respectively. These similar trends can be attributed to the negative surface charge of adsorbent that maybe the probable sites for the adsorption of ions and also high concentration H^+ ions in the solution in lower pH values. There is an intense competition between H^+ ions present in the aqueous solution and metallic cations (Pb^{2+}, Co^{2+}, and Ni^{2+}) for the attachment to the adsorbent active sites in these pH values, where the formers overcome the other metallic cations by repulsive electrostatic forces between H^+ cations and metallic ions. The results show that the uptake percentages of the metallic ions decreased after pH = 6. This can be attributed to the formation of OH^- ions complexes and the competition between hydroxide ions and metallic cations for relocating on the adsorbent active sites [38]. Based on the data reported in Fig. 6, pH = 6 can be considered as the optimum value for the removal of current metallic ions from aqueous solution using the prepared adsorbent from *Citrus limetta* leaves, and the corresponding adsorption efficacies were 97.084%, 95.62%, and 93.43% for Pb, Co, and Ni, respectively.

3.3 Effect of adsorbent dosage

The dosage of adsorbent plays a key role in the adsorption process since the adsorbent capacity for the removal of a definite concentration of an adsorbate (metal ions) can be determined through studying this parameter. The adsorbent dosage effect on adsorption efficiencies and

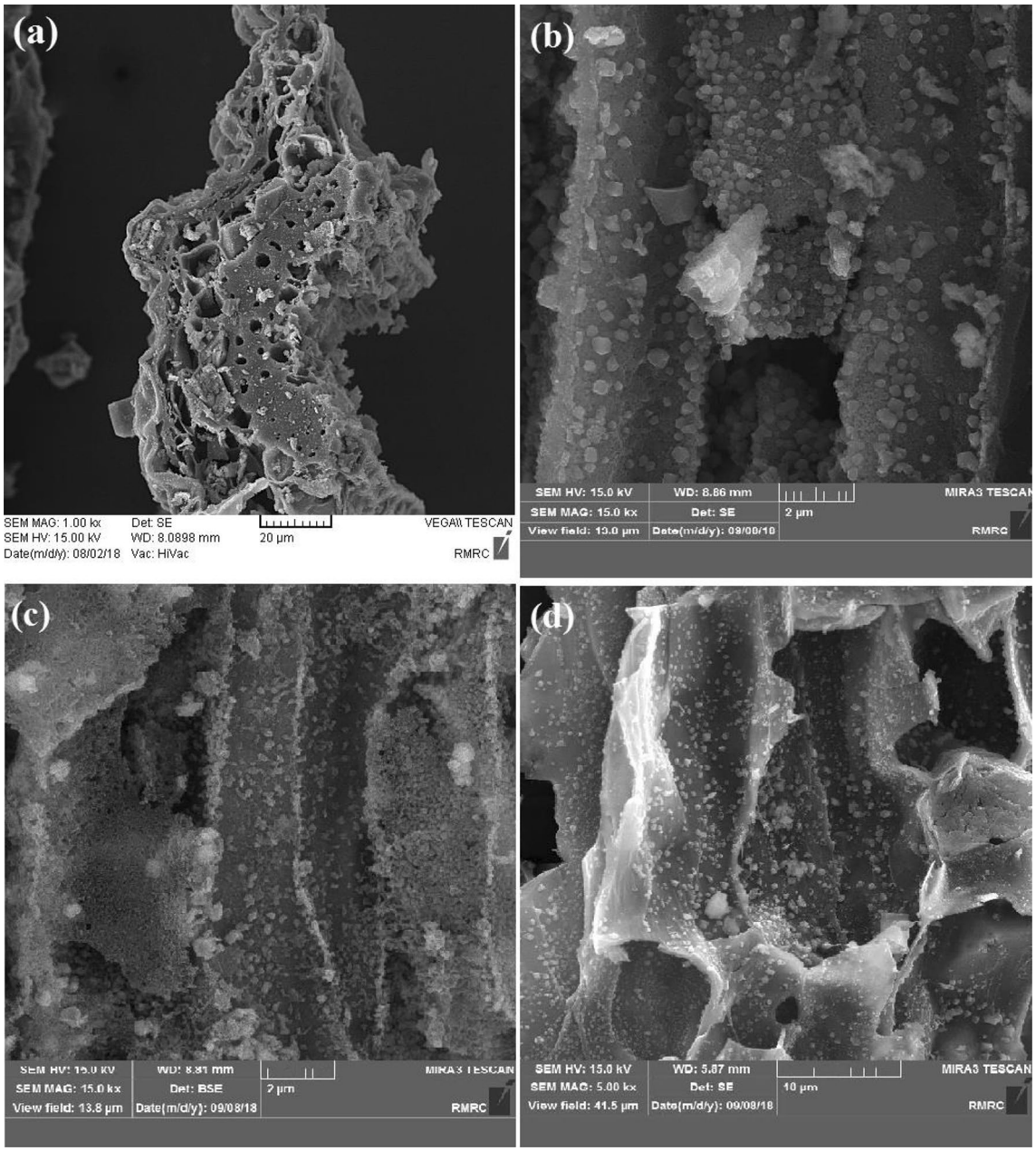

Fig. 2 SEM images of the activated carbon adsorbent prepared from *Citrus limetta* leaves: **a** before the adsorption of ions, **b** after the adsorption of lead ions, **c** after the adsorption of cobalt ions, and **d** after the adsorption of nickel ions

capacities of Pb(II), Co(II), and Ni(II) ions are shown in Fig. 7. Based on observations, adsorption efficiencies of lead (83.43–98.32%), Cobalt (82.78–96.33%), and nickel (80.62–94.41%) increased impressively in the adsorbent dosage range of 0.25–1 g/L. By increasing the adsorbent dosage, adequate active sites are accessible for the metallic ions, therefore they can easily diffuse and adsorb in the adsorbent structure, which results in higher adsorption values. As it can be seen, the diagram becomes constant behind the dosage of 1 g/L, since a small amount of ions remained in the solution. Therefore, the maximum adsorption efficiencies can be achieved in the adsorbent dosage of 1 g/L. On the other hand, based on the data presented in Fig. 7, the adsorption capacity decreased with the adsorbent dosage, because of lack of enough metallic ions in aqueous solution to be adsorbed on the activated carbon adsorbent active sites [39].

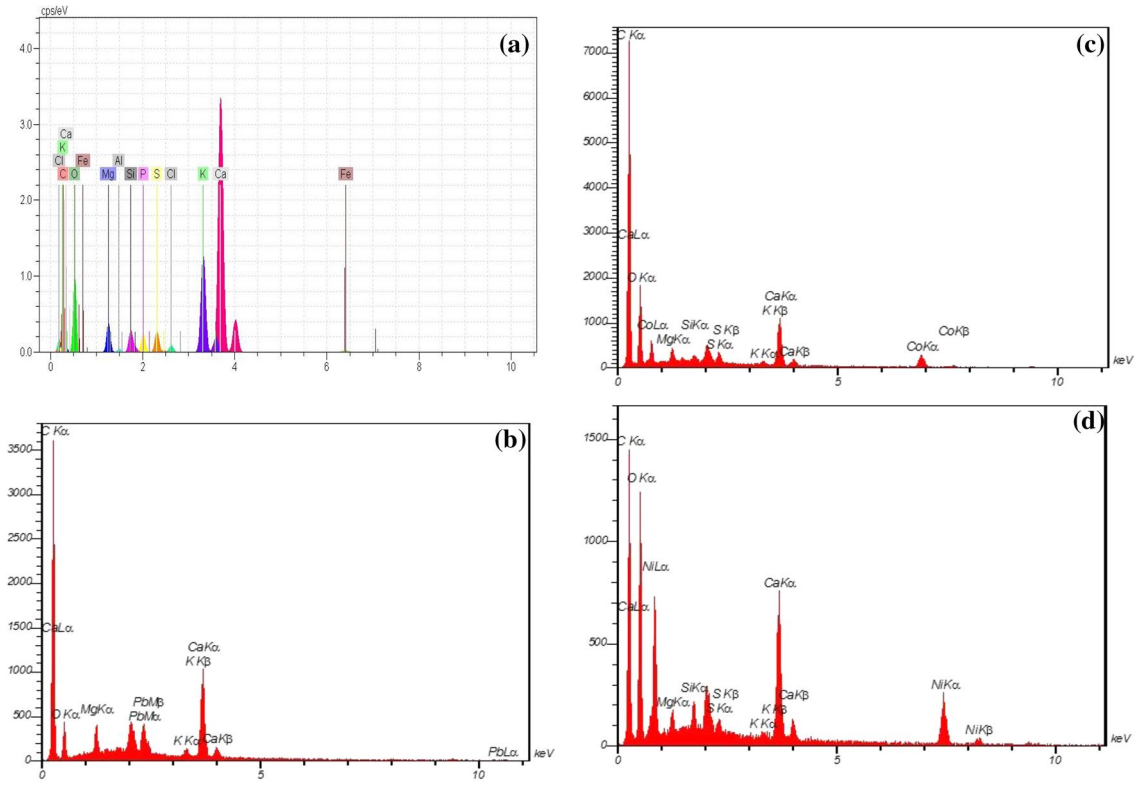

Fig. 3 EDX analysis of the activated carbon adsorbent: **a** before the adsorption of ions, **b** after the adsorption of lead ions, **c** after the adsorption of cobalt ions, and **d** after the adsorption of Ni ions

Table 1 Weight percentages of the activated carbon constituents prepared from *Citrus limetta* tree leaves before and after the adsorption of lead, cobalt, and nickel ions

Element (wt%)	Activated carbon	Adsorbent after Pb (II) adsorption	Adsorbent after Co (II) adsorption	Adsorbent after Ni (II) adsorption
O	40.26	17.82	26.68	37.46
Ca	25.19	8.14	3.76	6.33
C	19.27	67.05	63.17	43.95
P	8.13	–	–	–
Mg	2.10	1.50	0.74	0.63
Si	1.49	–	0.41	0.71
S	1.28	–	0.64	0.57
P	1.19	–	–	–
Fe	0.53	–	–	–
K	0.42	0.70	0.26	0.23
Al	0.14	–	–	–
Pb	–	4.79	–	–
Co	–	–	4.34	–
Ni	–	–	–	10.12
Total	100	100	100	100

3.4 Temperature effect

The other important parameter of the adsorption processes is the temperature that its effect on the adsorption efficiencies of lead, cobalt, and nickel ions is shown in Fig. 8. According to these data, adsorption efficiencies dropped with temperature in 25–50 °C. The current decline may be due to the ions tendency for the separation from the adsorbent surface

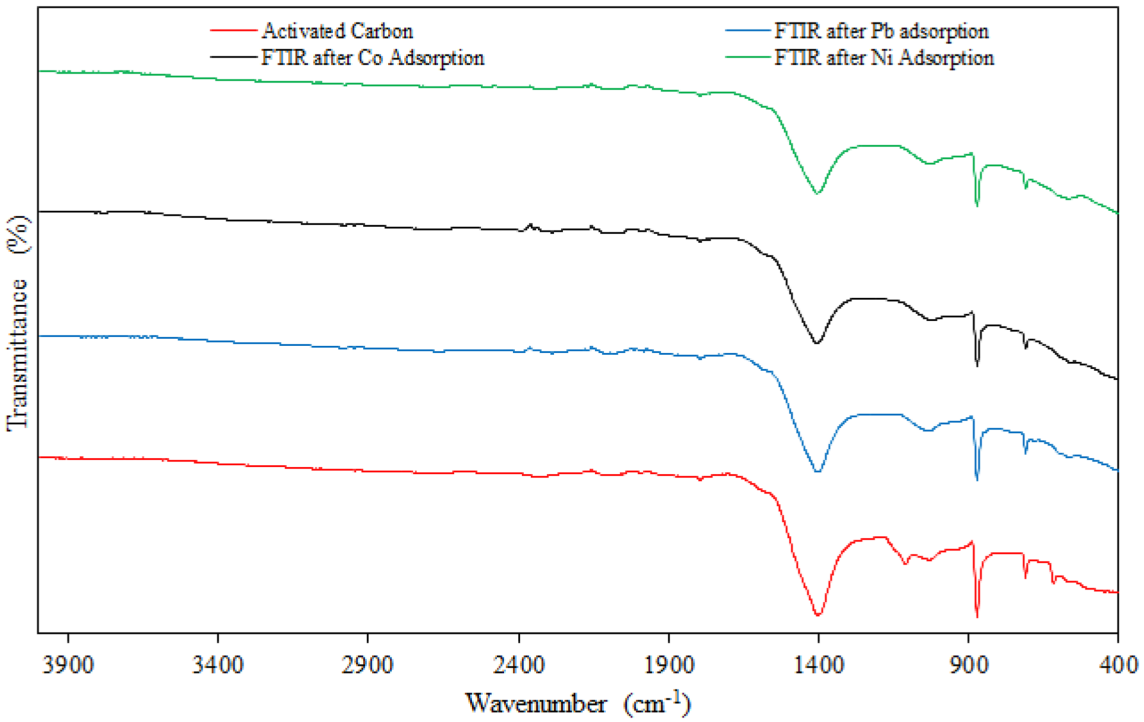

Fig. 4 FTIR spectra of the activated carbon prepared from *Citrus limetta* leaves before and after the adsorption process

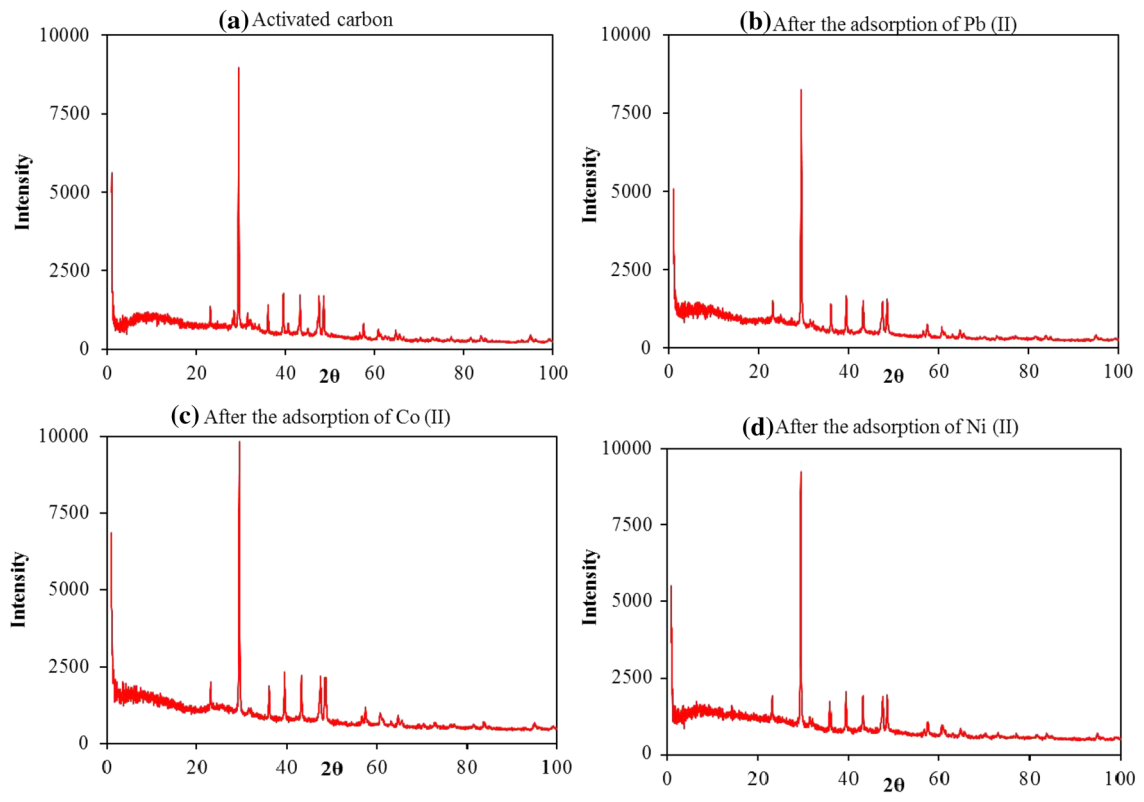

Fig. 5 XRD spectra of the activated carbon adsorbent prepared from *Citrus limetta* leaves: **a** before the adsorption of ions, **b** after the adsorption of lead ions, **c** after the adsorption of cobalt ions, and **d** after the adsorption of nickel ions

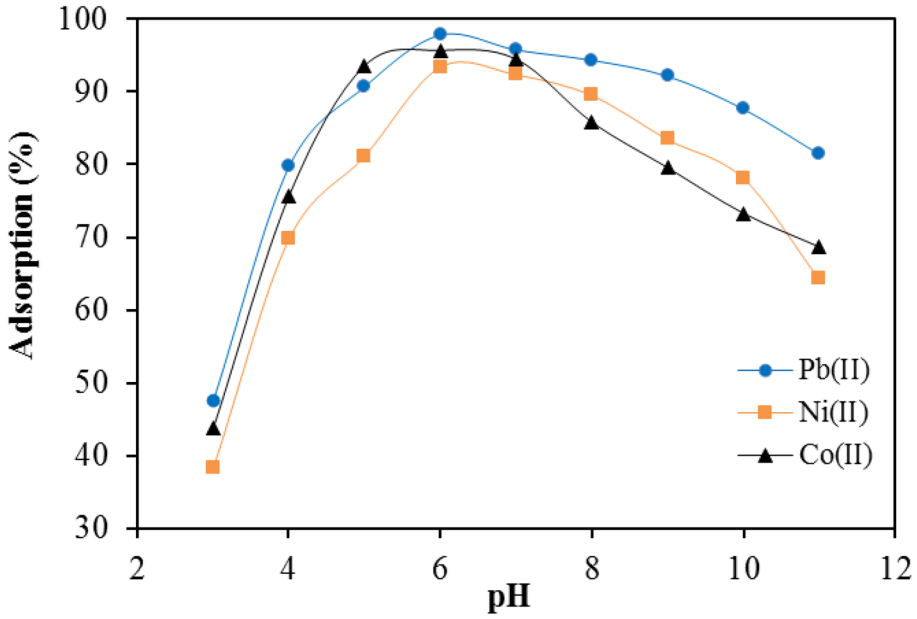

Fig. 6 Effect of solution pH on Pb (II), Co (II), and Ni (II) ions adsorption efficiencies using the activated carbon adsorbent prepared from *Citrus limetta* leaves (adsorbent dosage = 0.75 g/L, T = 25 °C, initial concentration = 10 mg/L, t = 60 min, and stirring rate = 200 rpm)

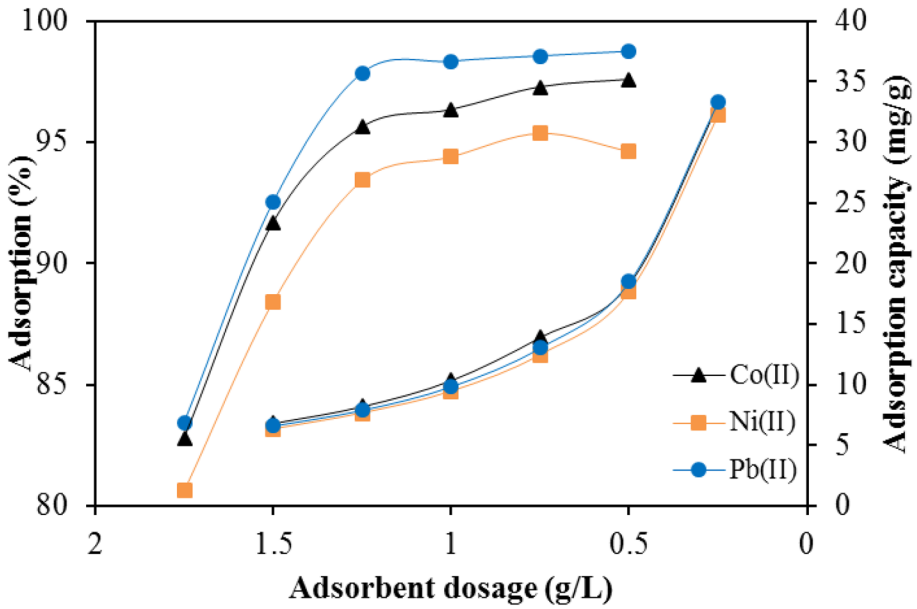

Fig. 7 Effect of adsorbent dosage on Pb (II), Co (II), and Ni (II) ions adsorption efficiencies and capacities using the activated carbon adsorbent prepared from *Citrus limetta* leaves (pH = 6, T = 25 °C, initial concentration = 10 mg/L, t = 60 min, and stirring rate = 200 rpm)

and returning into the solution as the result of temperature increase. Therefore, it can be said that adsorption processes of lead, cobalt, and nickel ions were exothermic and the optimum temperature to achieve the maximum adsorption efficiencies of these ions was 25 °C, in which the efficiencies of Pb(II), Co(II), and Ni(II) ions were 98.32%, 96.33%, and 94.41%, respectively.

3.5 Metal ions initial concentration effect

Figure 9 presents the effect of the initial concentration of Pb(II), Co(II), and Ni(II) ions in the range of 5–100 mg/L on the uptake percentage and capacity of the current adsorbent. This parameter is a significant component of the adsorption process since it supplies the essential mass transfer driving force between the solution and the adsorbent. It can be seen from the data in this figure that the maximum adsorption efficiencies for these ions were achieved in the concentration value of 5 mg/L since there were plenty of unoccupied active sites available on the surface of the activated carbon adsorbent in initial steps of the process, and therefore the concentration driving for the adsorption of Pb, Co, Ni ions were relatively high, which were followed by consequent high adsorption efficiencies as the result of probable collisions between the ions and the adsorbent surface. There is also a negative correlation

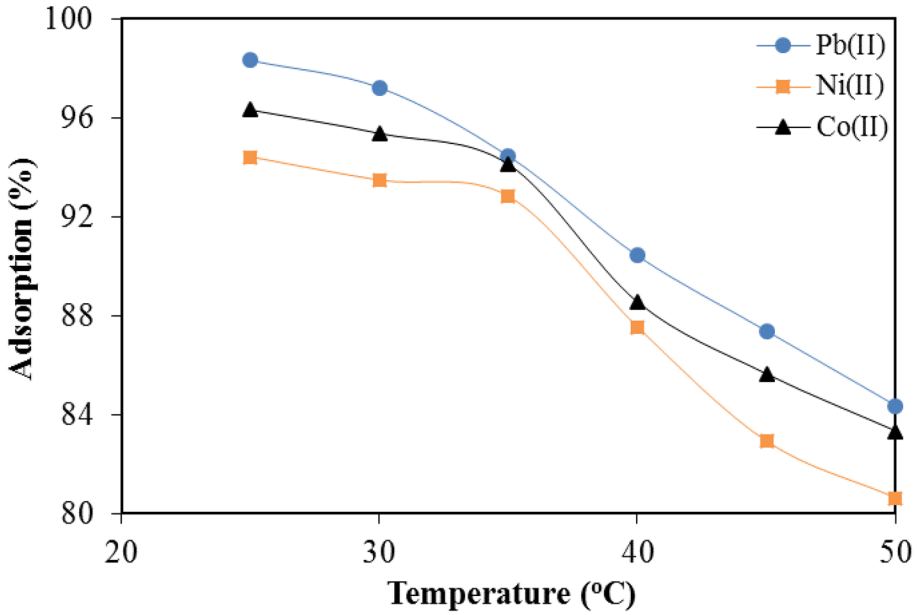

Fig. 8 Effect of temperature on Pb (II), Co (II), and Ni (II) ions adsorption efficiencies using the activated carbon adsorbent prepared from *Citrus limetta* leaves (pH = 6, adsorbent dosage = 1 g/L, initial concentration = 10 mg/L, t = 60 min, and stirring rate = 200 rpm)

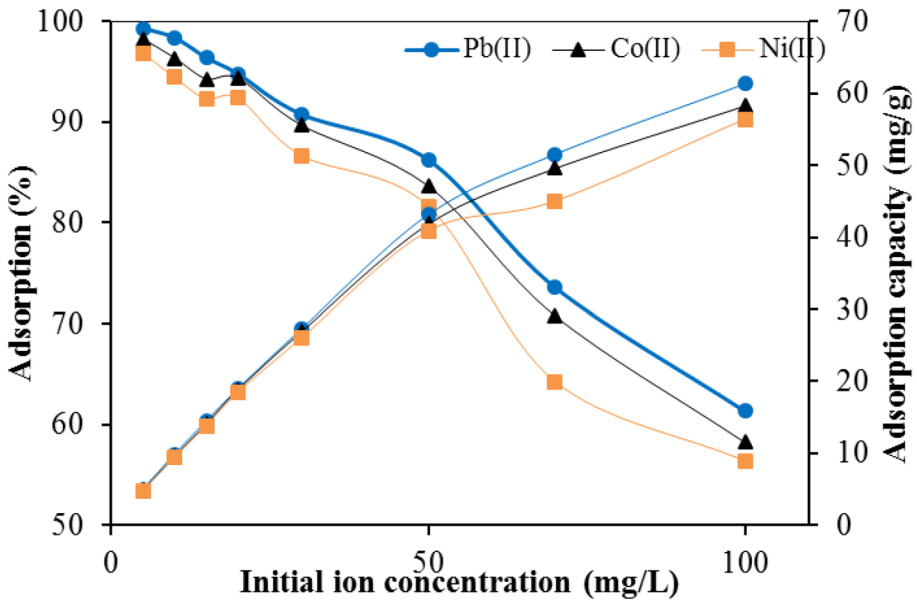

Fig. 9 Effect of Pb (II), Co (II), and Ni (II) ions initial concentration on their adsorption efficiencies and capacities (pH = 6, the adsorbent dosage of 1 g/L, T = 25 °C, t = 60 min, and stirring rate = 200 rpm)

between the ion concentration and their removal efficiencies for the concentrations higher than 5 mg/L, because of lack of an adequate number of available active sites for the adsorption of excess ions [40–42].

Additionally, it is apparent from Fig. 9 that adsorption capacity rose steadily by the ions concentration. This may be related to the high ratio of the number of ions in the aqueous solution to the number of active sites and functional groups of the adsorbent surface [43]. The results of the current research showed that the adsorbent capacity order of the activated carbon prepared from *Citrus limetta* leaves is as follows: Pb > Co > Ni.

3.6 Contact time effect

The effect of contact time on Pb(II), Co(II), and Ni(II) ions adsorption efficiencies in the time range of 5–120 min is shown in Fig. 10. As it can be seen, there is an initial steep rise in adsorption efficiencies of lead (99.25%), cobalt (II) (98.21%), and nickel (II) (96.82%) ions in the contact time range of 5–60 min, which shows high adsorption rates. This can be attributed to the abundance of vacancies and unoccupied active sites for the metal ions at the beginning of the process. After 60 min, the diagram gradually became constant and no significant further increase in the adsorption

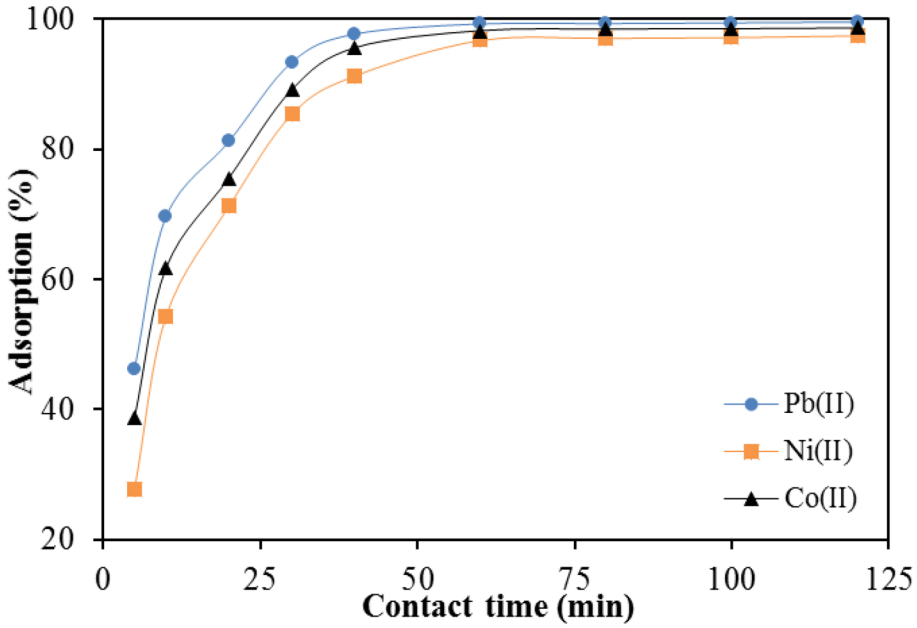

Fig. 10 Effect of contact time on Pb (II), Co (II), and Ni (II) ions removal efficiencies from aqueous solutions by the activated carbon adsorbent prepared from *Citrus limetta* leaves (pH = 6, adsorbent dosage = 1 g/L, T = 25 °C, initial concentration = 5 mg/L, and stirring rate = 200 rpm)

efficiencies of the ions was seen, because of saturation of prepared adsorbent active sites by the adsorbed ions. Therefore it can be concluded that contact time of 60 min can be considered as the optimum value for the adsorption of Pb(II), Co(II), and Ni(II) ions from the synthetic solution in the current conditions of the experiments.

3.7 Adsorption isotherms

Adsorption isotherms represent a function which is applied to relate the adsorbate concentration to the concentration of remaining impurities in the solution at a constant time and under equilibrium condition [16]. The linear form of Langmuir and Freundlich models were applied to describe the equilibrium behavior of Pb(II), Co(II), and Ni(II) ions adsorption. Langmuir isotherm is used to explain the single layer adsorption with a finite number of active sites. The linear from of Langmuir isotherm is as follows:

$$\frac{C_e}{q_e} = \frac{1}{q_m K_L} + \frac{C_e}{q_m} \tag{3}$$

In Eq. (3), C_e and q_e are the metallic ion equilibrium concentration in the liquid phase (mg/L) and the equilibrium adsorption capacity (mg/g), respectively. q_{max}, K_L are the adsorption isotherm constants that show the maximum adsorption capacity (mg/g) and adsorption energy (L/mg), respectively. The values of these two parameters can be determined from the slope and intercept values of q_e/C_e versus C_e plot. The adsorption intensity, R_L, which is the most important feature of Langmuir isotherm, is calculated by Eq. (4):

$$R_L = \frac{1}{1 + K_L C_i}. \tag{4}$$

The value of this parameter determines the adsorption process of nature. For $0 < R_L < 1$, $R_L > 1$, $R_L = 1$, and $R_L = 0$, the process is reversible and desirable, non-desirable, desirable and linear, and reversible, respectively [44].

As an experimental model, Freundlich isotherm describes the adsorption process on a heterogeneous surface. Equation 2 shows the linear form of the Freundlich isotherm model:

$$\ln q_e = \frac{1}{n} \ln C_e + \ln K_f, \tag{5}$$

where K_f (L/mg) and n are Freundlich model constants and denote the adsorption rate and degree of the adsorption process nonlinearity, respectively. These two parameters are determined from the values of slope and intercept of $\ln q_e$ versus $\ln C_e$ plot. It should be noted that the process is linear when n is equal to 1, and for n values lower and higher than 1, the process is linear chemical and physical, respectively [45, 46].

Figures 11 and 12 and Table 2 show the linear plots and parameters of Langmuir and Freundlich isotherm models for the removal of lead, cobalt, nickel ions from the aqueous solutions by the prepared activated carbon. According to these data, the values of R_L for Pb (II), Co(II), and Ni(II) ions were between 0 and 1. This means that their adsorption was desirable and reversible. Additionally, the maximum adsorption capacities for Pb(II), Co(II), and Ni(II) ions were 62.89, 60.60, and 58.13 mg/g, respectively, which are acceptable values for the prepared adsorbent. Furthermore,

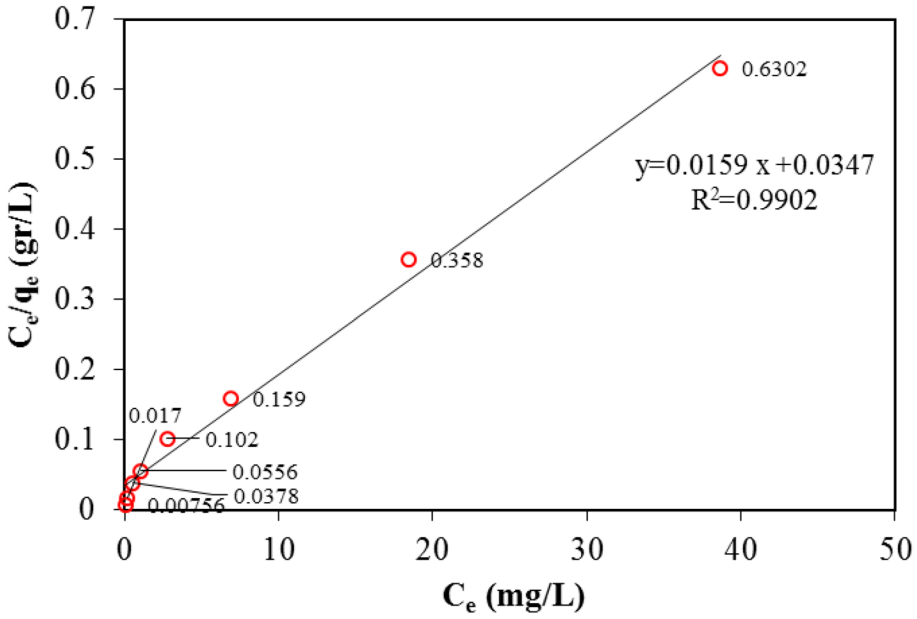

Fig. 11 Langmuir isotherm model diagrams for the adsorption of lead ions from aqueous solution by the activated carbon adsorbent prepared from *Citrus limetta* leaves (pH = 6, adsorbent dosage = 1 g/L, T = 25 °C, initial concentration = 5–100 mg/L, *t* = 60 min, and stirring rate = 200 rpm)

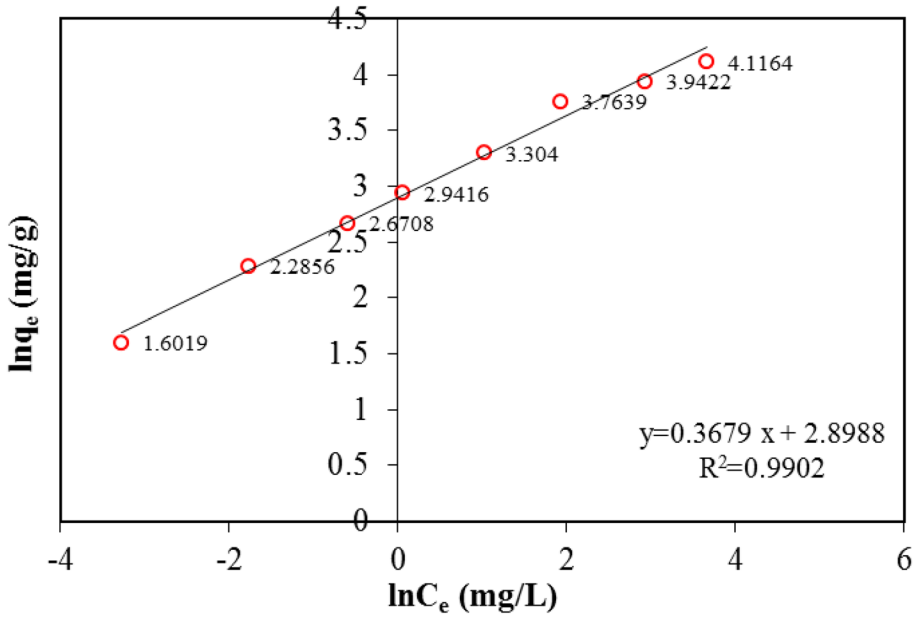

Fig. 12 Freundlich isotherm model diagrams for the adsorption of (a) lead ions from aqueous solution by the activated carbon adsorbent prepared from *Citrus limetta* leaves (pH = 6, adsorbent dosage = 1 g/L, T = 25 °C, initial concentration = 5–100 mg/L, t = 60 min, and stirring rate = 200 rpm)

Table 2 Langmuir and Freundlich adsorption isotherm parameters for the adsorption of lead, cobalt, and nickel ions by the activated carbon adsorbent prepared from *Citrus limetta* tree leaves

Models	Parameters	Pb (II)	Co (II)	Ni (II)
Langmuir	q_m	62.89	60.60	58.139
	K_L	0.458	0.2743	0.363
	R^2	0.9902	0.9933	0.9857
	R_L	0.303–0.0213	0.355–0.0268	0.421–0.0351
Freundlich	n	2.718	2.273	2.305
	K_f	18.15	15.38	12.7
	R^2	0.9902	0.9842	0.968

the correlation coefficient (R^2) of Pb(II), Co(II), Ni(II) linear forms were as 0.9902, 0.9857, and 0.9933, respectively. Based on these R^2 values, Langmuir model is capable of describing the adsorption equilibrium of these ions.

The values of parameter *n* which are presented in Table 2, were calculated equal to 2.718, 2.305, and 2.273 for lead, cobalt, and nickel, respectively. These $n > 1$ values show that the current adsorption processes were physical and desirable. In addition, R^2 values of Pb(II), Co(II), and Ni(II) Freundlich linear forms were 0.9908, 0.9842, and 0.968, respectively. Considering these correlation coefficients, it can be said that the Langmuir model performed better than Freundlich isotherm in the description of these ions adsorption equilibrium

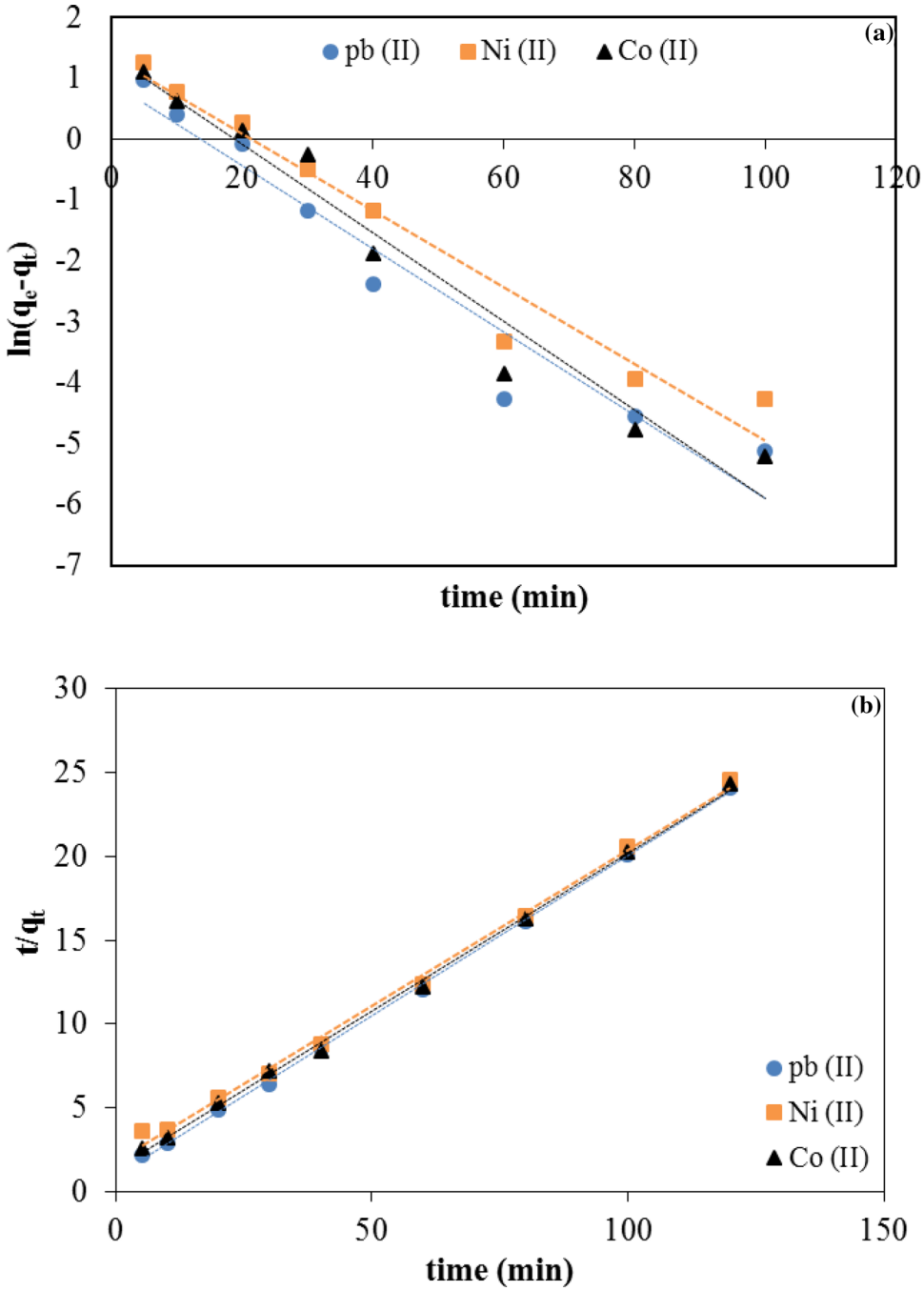

Fig. 13 **a** Pseudo-first-order and **b** pseudo-second-order kinetic model diagrams for adsorption of lead, cobalt, and nickel ions from aqueous solution by the activated carbon adsorbent prepared from *Citrus limetta* leaves

behavior. Therefore, the current adsorption processes were considered as single layer processes.

3.8 Kinetic study of adsorption

Kinetic studies can help to have a deep insight about the adsorption process by depicting the interactions at the solid-solution interface [47]. Pseudo-first-order and pseudo-second-order kinetic models have been applied to investigate the kinetics of Pb(II), Co(II), and Ni(II) ions adsorption process. The pseudo-first-order model is based on the hypothesis of the direct relation between the adsorption rate and the number of adsorbent active sites. Pseudo-first-order model linear form is shown as Eq. (6):

$$\ln\left(q_e - q_t\right) = \ln q_e - K_1 t \tag{6}$$

Table 3 Pseudo-first-order and pseudo-second-order kinetic model parameters for the adsorption of lead, cobalt, and nickel ions by the activated carbon adsorbent prepared from *Citrus limetta* tree leaves

Kinetic models	Parameters	Heavy metal ions		
		Pb (II)	Co (II)	Ni (II)
Pseduo-first-order	R^2	0.9392	0.9593	0.9583
	$q_{exp\ (mg/g)}$	4.9765	4.9315	4.877
	$q_{cal\ (mg/g)}$	2.511	3.9538	3.8694
	K_1	0.0683	0.0728	0.063
Pseduo-second-order	R^2	0.9993	0.9962	0.9983
	$q_{exp\ (mg/g)}$	4.9765	4.9315	4.877
	$q_{cal\ (mg/g)}$	5.23	5.37	5.299
	K_2	0.0387	0.019	0.0266

In this equation, q_t is the value of adsorbed ions (mg/g) at time t per gram of adsorbent and K_1 is the rate constant of pseudo-first-order model (min^{-1}). It should be noted that K_1 and q_e can be achieved from the values of slope and intercept of $\ln(q_e - q_t)$ versus t line. Pseudo-second-order kinetic model is based on the assumption that the rate of the process is limited by the chemical adsorption. In addition, it is hypothesized that adsorption occurs on the solid phase, where the rate of adsorption of impurities on the active sites is proportional to the squared of the number of unoccupied sites. Equation (7) shows the linear form of pseudo-second-order model:

$$\frac{t}{q_t} = \frac{1}{K_2 q_e^2} + \frac{t}{q_e}. \tag{7}$$

In this equation, K_2 is the rate constant of pseudo-second-order model ($g.mg^{-1}.g^{-1}$). It should be noted that q_e and K_2 can be calculated from the values of slope and intercept of t/q_t versus t line.

The results of kinetic studies for the adsorption of lead, cobalt, and nickel ions by the activated carbon prepared from *Citrus limetta* leaves are presented in Fig. 13 and Table 3.

According to R^2 values, the adsorption processes of Pb (II), Co (II), and Ni (II) heavy metal ion comply with the pseudo-second-order kinetic model. Additionally, the deviations of the predicted adsorption capacities from the real capacity values were lower for pseudo-second-order model in comparison with pseudo-first-order model.

3.9 Thermodynamic studies

Adsorption process spontaneous nature can be evaluated through the study of its thermodynamic parameters such as Gibbs free energy ($\Delta G°$), enthalpy ($\Delta H°$), and entropy ($\Delta S°$) changes, which are calculated based on equilibrium constant [48]. The adsorption equilibrium constant value (K_e) is determined by Eq. (8):

$$K_e = \frac{q_e}{C_e} \tag{8}$$

Using K_e, Gibbs free energy changes are determined by Eq. (9):

$$\Delta G^0 = -RT \ln K_e \tag{9}$$

According to Eq. (9), $\Delta G°$ is the Gibbs free energy (kJ/mol), R is the universal gas constant (8.314 J/mol K), and T is the absolute temperature (Kelvin). Using Eq. (10), the equilibrium constant can be shown as a function of temperature, enthalpy, and entropy changes:

$$\ln K_e = -\frac{\Delta H^0}{RT} + \frac{\Delta S^0}{R} \tag{10}$$

The values of $\Delta H°$ and $\Delta S°$ are obtained from the slope and intercept of $\ln K_e$ versus T^{-1} [49]. Figure 14 and Table 4 present the results of thermodynamic studies of lead, cobalt, and nickel ions from aqueous solutions by the activated carbon adsorbent prepared from *Citrus limetta* leaves.

According to reported results, the $\Delta G°$ values for Pb(II), Co(II), and Ni(II) in the temperature range of 298–328 K were negative, therefore, adsorption of these ions was possible and spontaneous processes. In addition, the enthalpy values were also negative, indicating that the current adsorption processes were exothermic. On the other hand, negative values of entropy changes denoted that there was a negative correlation between the temperature and the current adsorption efficiencies and the system irregularities, which can be inferred based on Le-chateliers principle.

4 Conclusion

In this research, the adsorption of Pb (II), Co (II), and Ni (II) ions using the activated carbon prepared from *Citrus limetta* leaves was studied. The prepared adsorbent was analyzed by various techniques such as BET, SEM, EDX, FTIR, and XRD. Also the effect of various adsorption important parameters including solution pH, the dosage of adsorbent, temperature, ions initial concentration, and adsorption contact time were studied on the adsorption performance of the prepared adsorbent. According to results, the best pH value for the adsorption of heavy metal ions was 6. The other optimum parameter as follows: adsorbent dosage = 1 g/L, T = 25 °C, initial ion concentration = 5 mg/L, and t = 60 min. Equilibrium studies showed that Langmuir isotherm performed better than Freundlich. In addition, it was shown that the adsorption of the ions was physical and desirable. Adsorption kinetic studies

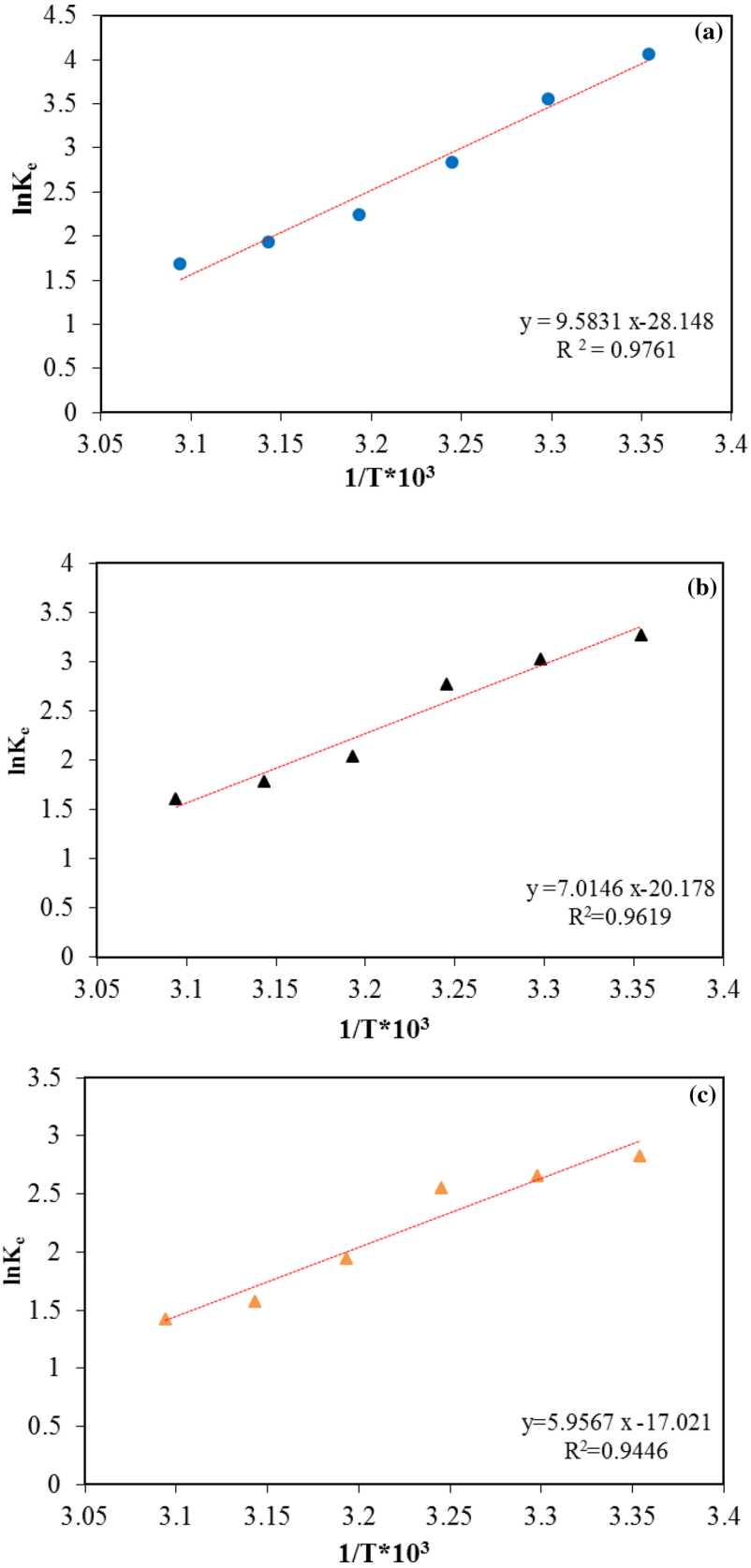

Fig. 14 Thermodynamic diagrams for the adsorption of **a** lead, **b** cobalt, and **c** nickel ions from aqueous solution by the activated carbon adsorbent prepared from *Citrus limetta* leaves (pH = 6, adsorbent dosage = 1 g/L, initial ion concentration = 10 mg/L, and *t* = 60 min)

Table 4 Thermodynamic parameters for the adsorption of lead, cobalt, and nickel ions from the aqueous solution by the activated carbon adsorbent prepared from *Citrus limetta* tree leaves

Heavy metal ion	Temperature (K)	Gibbs free energy (ΔG^0 = kJ/mol)	Entropy (ΔS^0 = J/mol)	Enthalpy (ΔH^0 = kJ/mol)
Pb(II)	298	−10.081	−234.02	−79.67
	303	−8.953		
	308	−7.257		
	313	−5.8413		
	318	−5.1155		
	323	−4.5276		
Co(II)	298	−8.0942	−167.75	−58.319
	303	−7.6264		
	308	−7.1005		
	313	−5.3203		
	318	−4.7187		
	323	−4.3192		
Ni(II)	298	−7.0033	−141.51	−49.52
	303	−6.7039		
	308	−6.5497		
	313	−5.0708		
	318	−4.177		
	323	−3.8312		

indicated that the experimental data were fitted by pseudo-second-order kinetic model. Finally, thermodynamic investigations denoted that the adsorption of lead, cobalt, and nickel ions by the prepared adsorbent was spontaneous and possible. Based on negative enthalpy values, it can be said that the processes were exothermic, while the negative entropy values meant that the current adsorption processes were followed by the decrease of irregularities.

References

1. Bakhtiari N, Azizian S (2015) Adsorption of copper ion from aqueous solution by nanoporousMOF-5: a kinetic and equilibrium study. J Mol Liq 206:114–118
2. Dashamiri S, Ghaedi M, Asfaram A, Zare F, Wang S (2017) Multi-response optimization of ultrasound assisted competitive adsorption of dyes onto Cu(OH)2-nanoparticle loaded activated carbon: central composite design. Ultrason Sonochem 34:343–353
3. Zhao F, Repo E, Yin D, Meng Y, Jafari S, Sillanpaa M (2015) EDTA-cross-linked beta-Cyclodextrin: an environmentally friendly bifunctional adsorbent for simultaneous adsorption of metals and cationic dyes. Environ Sci Technol 49:10570–10580
4. Nomanbhay SM, Palanisamy K (2005) Removal of heavy metal from industrial wastewater using chitosan coated oil palm shell charcoal. Electron J Biotechn 8:43–53
5. Kobya M, Demirbas E, Senturk E, Ince M (2005) Adsorption of heavy metal ions from aqueous solutions by activated carbon prepared from apricot stone. Bioresour Technol 96:1518–1521
6. Sheng PX, Ting YP, Chen JP, Hong L (2004) Sorption of lead, copper, cadmium, zinc, and nickel by marine algal biomass: characterization of biosorptive capacity and investigation of mechanisms. J Colloid Interf Sci 275:131–141
7. Meitei MD, Prasad MNV (2013) Lead (II) and cadmium (II) biosorption on Spirodela polyrhiza (L.) Schleiden biomass. J Environ Chem Eng 1:200–207
8. King P, Srinivas P, Kumar YP, Prasad VS (2006) Sorption of copper (II) ion from aqueous solution by Tectona grandis lf (teak leaves powder). J Hazard Mater 136:560566
9. Sekar M, Sakthi V, Rengaraj S (2004) Kinetics and equilibrium adsorption study of lead (II) onto activated carbon prepared from coconut shell. J Colloid Interf Sci 279:307–313
10. Fu F, Wang Q (2011) Removal of heavy metal ions from wastewaters: a review. J Environ Manag 92:407–418
11. Zhao X, Song L, He J, Wu T, Qin Y (2010) Adsorption characteristics of Ni^{2+} ion onto the diethylenetriaminepentaacetic acid-melamine/polyvinylidene fluoride blended resin. Int J Energy Environ 1:121–132
12. Kurniawan TA, Chan GY, Lo WH, Babel S (2006) Physico–chemical treatment techniques for wastewater laden with heavy metals. Chem Eng J 118:83–98
13. Wang YH, Lin SH, Juang RS (2003) Removal of heavy metal ions from aqueous solutions using various low-cost adsorbents. J Hazard Mater 102:291–302
14. Madhava Rao M, Ramana DK, Seshaiah K, Wang MC, Chang Chien SW (2009) Removal of some metal ions by activated carbon prepared from Phaseolus aureus hulls. J Hazard Mater 166:1006–1013
15. Fakhre NA, Ibrahim BM (2018) The use of new chemically modified cellulose for heavy metal ion adsorption. J Hazard Mater 343:324–331
16. Heiba HF, Taha AA, Mostafa AR, Mohamed LA, Fahmy MA (2018) Synthesis and characterization of CMC/MMT nanocomposite for Cu^{2+} sequestration in wastewater treatment. Korean J Chem Eng 35:1844–1853
17. Afkhami A, Saber-Tehrani M, Bagheri H (2010) Simultaneous removal of heavy-metal ions in wastewater samples using nano-alumina modified with 2,4-dinitrophenylhydrazine. J Hazard Mater 181:836–844
18. Demiral H, Güngör C (2016) Adsorption of copper (II) from aqueous solutions on activated carbon prepared from grape bagasse. J Clean Prod 124:103–113
19. Bouhamed F, Elouear Z, Bouzid J (2012) Adsorptive removal of copper (II) from aqueous solutions on activated carbon prepared from Tunisian date stones: equilibrium, kinetics and thermodynamics. J Taiwan Inst Chem Eng 43:741–749
20. Ding L, Zou B, Gao W, Liu Q, Wang Z, Guo Y, Wang X, Liu Y (2014) Adsorption of Rhodamine-B from aqueous solution using treated rice husk-based activated carbon. Colloids Surf A Physicochem Eng Asp 446:1–7
21. Yagmur E, Tunc MS, Banford A, Aktas Z (2013) Preparation of activated carbon from autohydrolysed mixed southern hardwood. J Anal Appl Pyrolysis 104:470–478
22. Fernandez ME, Nunell GV, Bonelli PR, Cukierman AL (2014) Activated carbon developed from orange peels: batch and dynamic competitive adsorption of basic dyes. Ind Crops Prod 62:437–445
23. Yang J, Yu M, Chen W (2015) Adsorption of hexavalent chromium from aqueous solution by activated carbon prepared from longan seed: kinetics, equilibrium and thermodynamics. J Ind Eng Chem 21:414–422
24. Mondal S, Sinha K, Aikat K, Halder G (2015) Adsorption thermodynamics and kinetics of ranitidine hydrochloride onto superheated steam activated carbon derived from mung bean husk. J Environ Chem Eng 3:187–195

25. Yuso AM, Rubio B, Izquierdo MT (2014) Influence of activation atmosphere used in the chemical activation of almond shell on the characteristics and adsorption performance of activated carbons. Fuel Process Technol 119:74–80
26. Saygılı H, Güzel F, Onal Y (2015) Conversion of grape industrial processing waste to activated carbon sorbent and its performance in cationic and anionic dyes adsorption. J Clean Prod 93:84–93
27. Goher ME, Hassan AM, Abdel-Moniem IA, Fahmy AH, Abdo MH, El-sayed SM (2015) Removal of aluminum, iron and manganese ions from industrial wastes using granular activated carbon and Amberlite IR-120H. Egypt J Aquat Res 41:155–164
28. Sezgin S, Ates M, Parlak EA, Sarac AS (2012) Scan rate effect of 1-(4-methoxyphenyl)-1H-pyrrole electro-coated on carbon fiber: characterization via cyclic voltammetry, FTIR-ATR and electrochemical impedance spectroscopy. Int J Electrochem Sci 7:1093–1106
29. Concha BM, Chatenet M, Coutanceau C, Hahn F (2009) In situ infrared (FTIR) study of the borohydride oxidation reaction. Electrochem Commun 11:223–226
30. Fernández-Francos X, Cook WD, Serra À, Ramis X, Liang GG, Salla JM (2010) Crosslinking of mixtures of DGEBA with 1,6-dioxaspiro[4,4]nonan-2,7-dione initiated by tertiary amines. Part IV. Effect of hydroxyl groups on initiation and curing kinetics. Polymer 51:26–34
31. Adebisi GA, Chowdhury ZZ, Alaba PA (2017) Equilibrium, kinetic, and thermodynamic studies of lead ion and zinc ion adsorption from aqueous solution onto activated carbon prepared from palm oil mill effluent. J Clean Prod 148:958–968
32. López T, Bosch P, Asomoza M, Gómez R, Ramos E (1997) DTA-TGA and FTIR spectroscopies of sol-gel hydrotalcites: aluminum source effect on physicochemical properties. Mater Lett 31:311–316
33. Dujardin C, Mamede AS, Payen E, Sombret B, Huvenne JP, Granger P (2004) Influence of the oxidation state of rhodium in three-way catalysts on their catalytic performances: an in situ FTIR and catalytic study. Top Catal 30:347–352
34. Yao S, Zhang J, Shen D, Xiao R, Gu S, Zhao M, Liang J (2016) Removal of Pb (II) from water by the activated carbon modified by nitric acid under microwave heating. J Colloid Interf Sci 463:118–127
35. Wang K, Zhao J, Li H, Zhang X, Shi H (2016) Removal of cadmium (II) from aqueous solution by granular activated carbon supported magnesium hydroxide. J Taiwan Inst Chem Eng 61:287–291
36. Saleh TA, Alhooshani KR, Abdelbassit MS (2015) Evaluation of AC/ZnO composite for sorption of dichloromethane, trichloromethane and carbon tetrachloride: kinetics and isotherms. J Taiwan Inst Chem Eng 55:159–169
37. Babarinde A, Onyiaocha GO (2016) Equilibrium sorption of divalent metal ions onto groundnut (Arachis hypogaea) shell: kinetics, isotherm and thermodynamics. Chem Int 2:37–46
38. Lawal OS, Sanni AR, Ajayi IA, Rabiu OO (2010) Equilibrium, thermodynamic and kinetic studies for the biosorption of aqueous lead (II) ions onto the seed husk of Calophyllum inophyllum. J Hazard Mater 177:829–835
39. Fan T, Liu Y, Feng B, Zeng G, Yang C, Zhou M, Zhou H, Tan Z, Wang X (2008) Biosorption of cadmium (II), zinc (II) and lead (II) by Penicillium simplicissimum: Isotherms, kinetics and thermodynamics. J Hazard Mater 160:655–661
40. Awual MR (2016) Ring size dependent crown ether based mesoporous adsorbent for high cesium adsorption from wastewater. Chem Eng J 303:539–546
41. Rafatullah M, Sulaiman O, Hashim R, Ahmad A (2009) Adsorption of copper (II), chromium (III), nickel (II) and lead (II) ions from aqueous solutions by meranti sawdust. J Hazard Mater 170:969–977
42. Bhakte NJ, Suryavanshi AA, Tirthakar SN (2015) Removal of heavy metal lead (pb) from electrochemical industry waste water using low cost adsorbent. Int J Res Eng Technol 4:731–733
43. Mahmoud ME, Kana MTA, Hendy AA (2015) Synthesis and implementation of nano-chitosan and its acetophenone derivative for enhanced removal of metals. Int J Biol Macromol 81:672–680
44. Cheng Q, Huang Q, Khan S, Liu Y, Liao Z, Li G, Ok YS (2016) Adsorption of Cd by peanut husks and peanut husk biochar from aqueous solutions. Ecol Eng 87:240–245
45. Siva Kumar N, Woo HS, Min K (2012) Equilibrium and kinetic studies on biosorption of 2,4,6-trichlorophenol from aqueous solutions by Acacia leucocephala bark. Colloid SurfB 94:125–132
46. Tong KS, Kassim MJ, Azraa A (2011) Adsorption of copper ion from its aqueous solution by a novel biosorbent Uncaria gambir: Equilibrium, kinetics, and thermodynamic studies. Chem Eng J 170:145–153
47. Zhao XH, Jiao FP, Yu JG, Xi Y, Jiang XY, Chen XQ (2015) Removal of Cu(II) from aqueous solutions by tartaric acid modified multi-walled carbon nanotubes. Colloids Surf A 476:35–41
48. Romero-Gonzalez J, Peralta-Videa JR, Rodríguez E, Delgado M, Gardea-Torresdey JL (2006) Potential of Agave lechuguilla biomass for Cr(III) removal from aqueous solutions: thermodynamic studies. Bioresource Technol 97:178–182
49. Aksu Z, İşoğlu İA (2005) Removal of copper (II) ions from aqueous solution by biosorption onto agricultural waste sugar beet pulp. Process Biochem 40:3031–3044